ENGINEERING RESEARCH INSTITUTE
THE UNIVERSITY OF MICHIGAN
ANN ARBOR

Final Report

THE EFFECTS OF SIZE AND SHAPE ON VISUAL DETECTION FOR CONTINUOUS FOVEAL TARGETS AT MODERATE BACKGROUND LUMINANCE

H. Richard Blackwell
A. B. Kristofferson

Vision Research Laboratories

ERI Project 2455

BUREAU OF SHIPS, DEPARTMENT OF THE NAVY
CONTRACT NO. Nobs-72038
WASHINGTON, D. C.

June 1958

ensm

UMR6450

The experiments reported here represent the basis for the doctoral dissertation:

"Foveal Intensity Discrimination as a

Function of Area and Shape"

by

Alfred B. Kristofferson

University of Michigan, 1954

TABLE OF CONTENTS

LIST OF FIGURES

LIST OF TABLES

SUMMARY

This paper presents a summary of experimental studies of the effects of target area and shape upon the detection of the eye, at 9.52 foot-lamberts back-ground luminance. The temporal forced-choice variant of the method of constant stimuli was utilized. Target presentation was foveal, with an exposure duration of 0.01 seconds. The targets were of uniform luminance, differing in area from 1 to 4096. square minutes, and in shape over a wide range of target types. A set of 60 targets was studied, intended to cover a very wide range with respect to target types to be expected in practical visibility situations. Three classes of non-circular targets were investigated: rectangles covering a wide range of areas and length-to-width ratios, multiple-legged figures (crosses, etc.), and a series of simple geometrical figures.

The data demonstrate that circular targets are more detectable for given area than any other target type studied. In general, the more non-circular a target, the less detectable is it in comparison with a circular target of equal area. This suggests the use of a "form factor" to allow for the non-circularity of targets in describing their visibility.

An effort has been made to derive empirical methods for analyzing the form factor required for different targets. We have found that form factor can be analyzed into three empirical factors relating to what are called "shape", "utilization", and "inhibition". These constructs have sufficient generality so that, utilizing them, the data for all targets studied are quantitatively ordered with a high degree of precision.

The data from these studies have also been analyzed in terms of a general theoretical formulation of the effects of target area and shape, designated the element contribution theory, which is described in detail elsewhere (Ref. 1). Essentially, this formulation states that a target is detected whenever it produces an amount of excitation at some point within its neural pattern which exceeds a critical value, E_c. Each point within the neural pattern receives excitation from every other point in an amount proportional to the distance, R, separating them. The amount of contribution as a function of distance is denoted by $\varphi(R)$. Thus, targets which are symmetrical and presented with their center at the point of fixation will be detected whenever the amount of excitation delivered to the center from all points stimulated by the target equals or exceeds E_c. The present experiments are restricted to targets which produce an excitation distribution having a single, centrally placed, peak of excitation. As explained in Ref. 1, the experimental program involves determining $\varphi(R)$ from the data for circular targets and using this information to predict the detectability of targets of non-circular shape.

SUMMARY (cont'd)

The general formulation was of considerable usefulness in ordering the experimental data but there was a clear need in addition for empirical factors of "asymmetry" and "utilization". There was little difference in the adequacy of ordering the data obtained for all targets with the three-factor empirical system or the two-factor empirical and theoretical system.

I. INTRODUCTION*

Since the initial observations by Ricco in 1877 (Ref. 3), many investigators have explored the effects of target area on detectability. In nearly every instance these studies utilized circular targets. In a few cases non-circular targets, usually rectangular in shape, have been used (Ref. 4,5,6,7). However, in no study have targets of different shape classes been compared in a comprehensive manner. It was the purpose of the studies reported here to do this.

A study of the effects of target size and shape is of obvious practical significance for predictions of the visibility of military targets, since the targets of military interest vary enormously with respect to these variables. The wide range of sizes and shapes of practical military targets suggests the desirability of obtaining a general understanding of the effects of target size and shape so that it will not be necessary to study a vast number of specific targets.

The present study was designed to provide such a general understanding of the effects of target size and shape. The targets studied were stylized so that geometrical descriptions are possible. The targets studied represent much more extreme cases of asymmetrical shape than will usually be encountered with practical military targets. The use of extremes of the target shape variable was intended to provide a stringent evaluation of the adequacy of descriptive systems developed on the basis of the present experiments.

A concerted effort has been made to develop general statements of the effects of target size and shape. Insofar as these provide adequate descriptions of the data from the present experiment, they should be very useful in predicting the visibility of military targets of practical interest.

II. PROCEDURES AND APPARATUS

All experiments were conducted in special experimental rooms, an artist's conception of which is shown in Figure 1. Two such rooms had to be used because the location of the Vision Research Laboratories was changed during the course of the experiments. The two rooms do not differ significantly as far as these experiments are concerned.

---

*This study was jointly sponsored by Project MICHIGAN, operating under Contract DA 36-039-sc-52654 between the U.S. Signal Corps and the University of Michigan. The Project MICHIGAN report of these studies has been made elsewhere (Ref. 2).

Only the uniformormly illuminated large white field produced by the inside of the cube was visible to the observers. A circular plastic screen 51 inches in diameter (25° degrees of visual angle at the average viewing distance) was located at the center of the field. The target was projected from a room at the rear of the cube onto the center of this translucent screen. In every case, observers had full knowledge of target position, shape, size and orientation. To aid the observer in fixing on the center of the target to be presented, four points of light were projected on the screen in a symmetrical pattern with respect to the target. Each orientation light subtended one minute of arc and each was located 18 minutes from the nearest point on the target. In other experiments we have shown that the 18 minute separation is sufficient to eliminate interaction effects for spatial configurations similar to the orientation light pattern used here. The intensity of the orientation lights was approximately ten times their threshold luminance. This luminance is the dimmest which is comfortable when used for fixation and orientation continuously.

Three female laboratory technicians and one of us (ABK), all between 20 and 30 years of age, served as observers. All, except observer NS, were previously experienced in the experimental procedures. Observer NS's inexperience was reflected in her initial data, the earliest of which were discarded. With the exception of these few data, observer NS provided over-all results of satisfactory stability.

Since the observers did not differ widely in sensitivity it was always possible for all four to serve simultaneously. When an observer was absent, the experimental sessions were repeated in order to obtain data for all observers under all stimulus conditions.

Measurements of refractive error were made under the constant viewing conditions of the experiments, using stigmatoscopic techniques. Lenses were prescribed for observers LP and AM which resulted in adequate correction. Observers AK and NS required no corrections.

Observers AK and AM were assigned permanent front seats, and NS and LP rear seats in the experimental rooms. The average viewing distance from eye to screen was 114 inches for the front seats, and 144 inches for the rear seats.

Target exposure duration was 0.010 seconds for all experiments. This duration is brief enough so that eye-movements cannot occur during a target presentation, and so that detection presumably represents a single neural event. Long exposure durations might be expected to result in more complex relations between target area and shape, and target detectability, than those obtained in these experiments.

A relatively constant, moderately high background luminance was maintained. Background and target luminances were measured independently before and after each experiment by standard visual photometric

techniques. From day to day the background luminance, B, ranged from 8.35 to 12.41 foot-lamberts, the average being 9.52 foot-lamberts. To simplify data reduction, threshold measurements were normalized to the mean background luminance. This normalizing process involved computing the change in threshold contrast attributable to background changes from the systematic, highly comparable data previously reported (Ref. 8). The only assumption involved is that individual differences in the slope of the threshold contrast-background luminance function are negligible over the range relevant here. The latter data (Ref. 8) are average data for two observers. This correction amounted to very little for the normal day-to-day background variations, the maximum correction being 5.1%. However, during one period of the experiments, that in which the series of rectangular targets was run, a calibration error resulted in the average background luminance being 23.3 foot-lamberts. These data were normalized to 9.52 foot-lamberts in the same way, the maximum correction being 41%.

All experiments employed the temporal forced-choice psychophysical method which has been described in detail in previous articles (Ref.9), wherein is contained data concerning the reliability of the method and its validity as a measure of sensory function. Essentially, the task assigned the observer is to identify in which of four immediately successive time intervals the visual target is presented. The four time intervals are set off by auditory signals and are immediately successive. Following each trial, or block of four time intervals, each observer is allowed sufficient time to indicate his choice of the "correct" interval by pressing one of four buttons on a concealed response box at his side. The time interval in which the target appears is determined at random and controlled automatically by a pre-punched program (Ref. 10).

Each target was presented many times at each of five luminance levels which were about equally spaced over the threshold range. These levels were obtained by inserting appropriate neutral density filters in the optical path so that the luminance of the target varied between that at which approximately 95% correct responses and that at which approximately 25% correct responses are obtained. Obviously, in the forced-choice method when the probability of target detection is zero, the probability of a correct response is 0.25. By plotting the target luminance against the percent of correct responses, threshold luminance was determined by interpolation at the 62.5% correct level. This process is described in greater detail below. All filters were calibrated periodically on an optical bench photometer.

A target was presented ten times at one luminance level, then at another, and so forth, the order of the blocks of ten being determined at random. A coded auditory signal informed the subjects of the luminance level to be presented next. The entire threshold determination for each target consisted of 250 presentations of the target in five groups of five blocks of ten trials. Each group contained every luminance level. Thus, the data for each threshold determination consisted of the

number of correct responses out of fifty at each of five target luminance levels, for each observer. A single threshold determination required about one and one-quarter hours of observing time. Usually, only one session was held each day.

The data were recorded automatically on punched cards as described in a previous article (Ref. 10), which also describes in detail the apparatus used for program scheduling and control of presentations.

The optical system of the target projector is shown schematically in Figure 2. Target size and shape were determined by a plate containing a cutout of the target. The plate was placed in the center of the projector beam, flush against the rear of the plastic screen. This produced a positive target with sharp edges on the front surface of the screen, the amount of edge blurring being less than four seconds of arc.

The target configurations fall into four groups: circles, rectangles (including squares), multiple-legged targets, and simple, regular geometrical figures. These classes of targets were run in the chronological order indicated in Table I.

Inasmuch as all data are to be compared with data on circular targets, targets of this shape were distributed throughout the experiments. In this way changes with time, such as practice effects, could be observed and taken into account. There were seven basic circular targets (an eighth was used on one occasion). For the observer in the near seats, the diameters of these circles subtended angles of about 1, 2, 4, 8, 16, 32, and 64 minutes of arc at the fovea.

Seven squares and twenty-one rectangles were used. The dimensions of these figures were chosen so that the areas of the squares were equal to those of the circles. The squares were run twice, once before and once after the other rectangles. Thresholds were determined for each rectangle oriented both horizontally and vertically. Length-to-width ratios varied from one to 64.

Samples of the multiple-legged figures can be seen in Figure 3. These figures consisted of crosses made up of 1x64 minute of arc rectangles arranged with the angle between the legs varying from 10° to 90°, a three-legged figure made up of three 1x32 segments, and six-legged figure composed of 1x64 segments. The spokes, shown in the bottom row of Figure 3, consisted of one minute wide rectangular segments added to a four minute diameter central circle. Two, four, and eight-legged spokes were run. The angle between legs of the four-legged spokes was varied from 10° to 90°. Two complete series of spokes were run, one with an over-all length of 32 minutes, the other of 64 minutes.

The six non-circular geometrical figures are displayed in Figure 4. They were constructed to be equal in area to the 32 minute diameter circular target, which was also run as part of the series.

Overall, the four observers each observed all of the 60 targets. The total number of responses was 130,000.

The data will be presented in terms of threshold contrast, $\mathring{C}$, which is defined as:

$$\mathring{C} = \frac{\mathring{\Delta B}}{B}$$

in which $\mathring{\Delta B}$ is the target luminance above background, B, corresponding to a detection probability of .50. The computation of $\mathring{\Delta B}$ involves adjusting the percent of correct answers at each target luminance level for the probability of a correct answer by chance, .25, and fitting a normal ogive to the corrected data. This procedure is described elsewhere (Ref. 11). For each set of threshold data, a chi-squared test of goodness of fit to the normal ogive is obtained. The results of this test are summarized in Table II for all experiments. One set of data accounts for much of the large chi-squared in the case of observer AM. If this one set of data (an 8-minute diameter circle) is omitted, the chi-squared sum for this observer becomes 366.78 with 345 degrees of freedom. This value has an associated probability of .20. The over-all goodness of fit of the ogives is considered to be excellent.

III RESULTS

Some significant differences between the four observers exist in the data. Analysis of the data for circles indicates that observers LP and AM had consistently lower thresholds than either observers AK or NS. Furthermore, observer NS had a lower threshold for small diameter circles, and a higher threshold for large diameter circles, than did observer AK. All of the data were analyzed in detail for the individual observers. There were no differences in the conclusions reached in comparing circular and non-circular targets. Therefore, to facilitate exposition, and to make the data available in the most useable form, they will be presented as average logarithmic values throughout the following discussion.

The experiments extended over a long period of time and small average differences in threshold appeared for each observer from period to period. For this reason, adjustments were made by bringing all of the data to the average sensitivity level of the Series 2 circular targets. This was accomplished for each observer by fitting a smooth curve to the data for circular targets, as discussed below, adjusting it so that the average deviation of the Series 2 circular targets was zero, and computing the average deviation of circular targets from the values given for them by the curve for each of the major time periods. The largest correction factor obtained in this was was -0.153 log units for observer NS during the initial series of circular targets and the average factor for all observers was -0.035 log units. All targets, including the non-circular ones, were adjusted by the most appropriate

correction factor.

The data from the four observers were combined in the following way. For circular targets, after the adjustment discussed in the preceeding paragraph, the mean of the threshold values read from the four curves was computed for the mean target area for each target. The obtained data was averaged for each target by taking the mean value of the deviation of the data point from the curve for each observer. This mean deviation was then expressed with respect to the average smooth curve. A similar procedure was used for the data for non-circular targets.

A. Circular Targets

A total of 90 separate threshold determinations were made for circular targets, divided approximately equally among the four observers and distributed throughout the area range for each observer. A smooth curve, required to have an orderly first derivative, was fit to the log area versus log threshold contrast plot for each observer. In Table III these data are summarized as averages over observers and over replications of targets. Table III, and the graphical plot of these data in Figure 5, are based on 22,500 observations. In Table III, $\log \mathring{C}_c$ is the average log threshold contrast determined by the smooth curves, and $\log \mathring{C}$ is the average obtained log threshold contrast. The algebraic average deviation of $\log C$ from $\log \mathring{C}_c$, hereafter denoted $\bar{\varepsilon}_c$ and defined as $\Sigma(\log \mathring{C} - \log \mathring{C}_c)/N$, is -.000. The absolute average deviation, $|\bar{\varepsilon}_c|$, defined as $\Sigma|\log C - \log \mathring{C}_c|/N$, is .006, or less than 2%.

The "area function" for circular targets, Figure 5, is of the general form usually found. Below a target diameter of about 2.8 minutes, area and threshold contrast are reciprocally related, i.e., Ricco's law holds. Above this "critical angle", area makes a continuously decreasing contribution to detectability.

B. Rectangular Targets

Each of the 28 rectangular targets was studied twice. For those with a dimensionality, viz. length-to-width ration, greater than unity, the targets were run once with the longer dimension, β, oriented vertically and once with β horizontal. There was no systematic difference between the vertical and horizontal orientations, hence they were averaged for each observer, and each threshold value in Table IV is an average of at least eight individual measurements. The data in Table IV are a summary of 77,000 responses.

Table IV contains the nominal target dimensions in the first column, and the exact dimensions in columns two and three, where α is the shorter dimension in minutes of arc. The threshold contrast for a circular target of the same area, A, as each rectangular target, is given in column six, denoted $\mathring{C}_c$. The threshold contrast predicted by

the element contribution hypotheses, $\mathring{C}_t$, appears in the last column and will be discussed in a later section.

Plotted in the same manner as the area function, the data for rectangular targets appear in Figure 6 in which the numbers indicate dimensionality and the smooth curve is the area function for circular targets from Figure 5. In general, the rectangular targets have higher threshold contrasts than circular targets of the same area, the extent of the difference being a function of dimensionality and being little affected by area within a narrow, middle range of areas. The loss in detectability due to increasing dimensionality is indicated by the average log unit difference between the obtained threshold contrast and the threshold contrast for a circular target of the same area, for a given dimensionality. Figure 7 summarizes these data from this point of view. It is clear that "form factor", or the loss in detectability associated with dimensionality, $\bar{\epsilon}_c$, is a negatively accelerated function of dimensionality, reaching a maximum of 0.41 log units at 64, the largest dimensionality studied. The smooth curve fitted through the data in Figure 7 is empirical.

C. Multiple-legged Targets

The cross targets were all constructed of 1x64 rectangles, but varied in the number of legs, having either three, four or six legs. Of the four-legged crosses, the angle θ between legs assumed several values: 10°, 22.5°, 24°, 60°, and 90°. These target characteristics are given in column one of Table V.

The spoke targets were similar, except that the number of legs were either two, four or eight, with angles θ of values indicated in Table V. The over-all length of the targets was 32 minutes in one series and 64 minutes in the other.

Entries in Table V are the same as in Table IV, with one exception. The shorter and longer dimensions of the targets α and β in this case refer to the dimensions of the rectangle which exactly encloses the multiple-legged target, and are denoted α' and β'.

Figure 8 displays the data, again with respect to the area function. The numbers indicate the over-all length of the target, either 32 or 64 minutes. The data for four-legged targets were averaged and appear in the figure as a single point for crosses, one for 1x32 spokes, and one for 1x64 spokes. Inspection of log C values in Table V reveals little difference attributable to the angle between legs. Clearly, non-circular targets of this class are less detectable than circular targets of the same area, $\bar{\epsilon}_c$ being 0.25, 0.38, and 0.48 for the 1x32 spoke, 1x64 spoke and 1x64 cross targets, respectively.

D. Geometrical Figures

These targets, which were relatively large and equal in area, differed extensively in shape. However, they differed little in

detectability, as an examination of the log Ć values in Table VI clearly indicates. In Table VI, α' and β' have the same meaning as they did in Table V. The average log Ć for the six targets is -1.084, while for a circular target of the same area log Ć is-1.118, a difference of only .034 log units, or 8%. This difference is in the same direction as for the other target classes.

All non-circular targets studied support the general conclusion that non-circular targets are less detectable than circular targets of the same areas This conclusion is illustrated by Figure 9 which is a summary of all the data plotted in terms of ϵ_c . The average difference is 0.169 log units, contributed mostly by the multiple-legged targets as indicated in Table VII, which gives $|\bar{\epsilon}_c|$, the mean of the absolute values of ϵ_c , and $\bar{\epsilon}_c$ for each of the four target classes.

IV. AN EMPIRICAL SUMMARY

A number of methods of summarizing the data have been tried. All have attempted to account for the variance in the data in terms of simple geometrical characteristics of the targets, and have been guided by general theoretical considerations. One method has emerged which is superior to all others tried. It will be described in this section.

We begin by considering ϵ_c values for the sample of rectangular targets. These values can be ordered in terms of a variable (D/α), where D is the target dimensionality (length-to-width ratio) and α is the linear extent, in minutes, of the smaller dimension of the target. Note, in Figure 10, that ϵ_c, the loss in detectability due to shape, increases as (D/α) increases beyond a value of approximately 1. This variable orders the data much better than simple dimensionality alone. From this analysis we may extract a shape correction (S), which is described by:

$$S = .25\,[\log (D/\alpha)] - .020 \qquad (2)$$

The S correction should be applied to all targets and it may then be determined what further order can be found in the residual ϵ_c, or ϵ_c', values.

For multiple-legged and geometrical form targets, the S-correction is based upon the dimensions of the smallest rectangular box into which the targets can be fitted. Examination of the multiple-legged targets in this way revealed one primary additional ordering trend, and one secondary one. The primary ordering trend concerns the extent to which the target "utilizes" the area of the rectangular box into which it just fits. In terms of target geometry, this is expressed

by $(A/\alpha'\beta')$, where A is target area, and α' and β' are the dimensions of the box. The secondary ordering trend concerns the extent of "inhibition" of parts of the target upon each other, measured by the angular separation between adjacent legs of the multiple-legged targets, denoted by θ. The functions in terms of $(A/\alpha'\beta')$ and θ were determined reiteratively in the following manner. To the data for all two-legged and four-legged, 90°, multiple-legged figures a function was fit to ϵ_c' versus log $(A/\alpha'\beta')$. These data were found to be ordered according to the function

$$U = -.33\ [\log\ (A/\alpha'\beta')] - .033. \qquad (3)$$

then, equation (3) was applied to all multiple-legged target data, yielding values of ϵ_c'', the values adjusted for both (D/α) and $A/\alpha'\beta'$). These proved to be ordered in terms of log θ as shown in Figure 11. The resulting equation is:

$$I = -.15\ (\log\ \theta) + .29\ . \qquad (4)$$

Finally, all of the ϵ_c' values were adjusted according to equation (4), resulting in ϵ_c'' values representing ϵ_c adjusted for S and I. These, plotted against log $(A/\alpha'\beta')$, fit the previously established equation (3) adequately, as can be seen in Figure 12.

Thus, four factors have been extracted from the data. Target detectability depends on area, in terms of the area function for circular targets, on shape as described by equation (2), on the extent to which the target utilitizes the area it "occupies" in the sense of equation (3), and on the angular separation of parts of the target according to equation (4). If each of our four targets classes are adjusted in accordance with those factors relevant to it, the results are as contained in Table VIII. This table also indicates which adjustments were applied to each target class. These residual errors are arrayed in Figure 13 as a function of log area for each of the 60 targets. The over-all average residual error is .037 log units, or 9%.

V THEORETICAL ANALYSIS

For each non-circular target, the value of threshold contrast predicted by the element contribution hypothesis was computed from the threshold contrasts for circular targets by the method of integration described previously (Ref.1). This procedure was carried through on the data for each observer individually, but will be presented here in terms of averages, since, again, the over-all pattern is highly similar for the different observers. The average values of predicted log threshold contrast are given in the righthand column of Tables IV, V and VI for each of the non-circular targets.

In the following discussion ϵ_t, log obtained threshold contrast

minus log predicted threshold contrast, will be the quantity of interest. Average values of ϵ_t, $\bar{\epsilon}_t$ and $|\bar{\epsilon}_t|$, are summarized for each target class in Table IX. For circular targets, ϵ_t , and ϵ_c , are identical, $|\bar{\epsilon}_t|$ providing a standard against which evaluation of the adequacy of prediction of the theory can be made. All targets are summarized in Figure 14 with respect to ϵ_t .

Over-all, the theory performs deceptively well, the grand algebraic mean of the ϵ_t values being .007 log units, or less than 2%. However, inspection of Table II suggests that this result is to some extent an artifact of the sample of targets which was chosen. On the whole, rectangular targets have thresholds lower than predicted and multiple-legged targets have thresholds higher than predicted. The extent to which the theory reduces the average error of prediction can be demonstrated by comparing .065, $|\bar{\epsilon}_t|$ for all non circular targets, with .191, $|\bar{\epsilon}_c|$ for non circular targets, and .006, $|\bar{\epsilon}_c|$ for circular targets. In terms of these log unit deviations, the theoretical predictions account for 64% of the error. That is, the prediction of threshold contrast for non-circular targets on the basis of the theory is a 64% improvement over prediction on the basis of the area function alone.

There are systematic trends in the errors of prediction within target classes. The rectangular targets are more detectable than predicted and the error of prediction increases as the rectangles become longer and thinner. Figure 15 shows that ϵ_t increases in the negative direction as (β-α), the difference between the longer and shorter dimension, increases. This "asymmetry" variable does the best job of ordering the ϵ_t values. The line represents the relation

$$A = - .003 (\beta - \alpha). \qquad (5)$$

For the most extreme rectangular target, ϵ_t is - .18 log units.

Following the same procedure as in the preceeding empirical analysis, the ϵ_t values for all multiple-legged targets were adjusted in accordance with equation (5) and one additional ordering trend became apparent, indicated in Figure 16. As in the empirical analysis, utilization was found to be a significant second-order effect. The following equation resulted:

$$U = .12 [\log (A/\alpha'\beta')] - .012 \qquad (6)$$

in which $(A/\alpha'\beta')$ is the percentage of the area of the best fitting rectangular box occupied by the target.

The residual errors of prediction after adjustment according to equations (5) and (6) are given in Table X and Figure 17. Comparison of Table X and Table VIII reveals little difference in the outcomes of the empirical and the theoretical-empirical analyses, the former having a slight advantage in the extent to which it orders the data of these experiments. The theoretical analysis, of course, has the advantage of greater generality.

VI. DISCUSSION

These experiments have shown that target area, in terms of visual angle, is a major factor determining target detectability. In addition, target shape has been shown to influence detectability to a significant extent, but in a complex manner. Maximal ordering of the data required extracting three factors related to target shape: dimensionality, utilization and inhibition. These terms are almost wholly descriptive at the present stage of research; the factors are defined by equations (2), (3) and (4).

A general formulation of the effects of target size and shape, the element contribution hypothesis, has been tested through these experiments and has been found to account for the effects of target shape to a significant extent. However, reliable second-order departures from theoretical prediction have been clearly defined, indicating that as target dimensionality increases, detectability becomes greater than expected theoretically and that as the extent to which a target "utilizes" the area surrounding it decreases, target detectability becomes less than the theory predicts. These factors are defined by equations (5) and (6).

Several possible revisions and extensions of the element contribution theory have been entertained to account for the observed departures. The theory assumes that $\varphi(R)$, the element contribution function, is independent of θ, the direction from the center. Since all rectangular targets were oriented only vertically and horizontally, it is possible that the A-function, equation (4), is due to a violation of this assumption. A brief series of experiments which determined threshold contrast for the 1x64 rectangular target in several orientations other than vertical and horizontal clearly eliminates this possibility. There is a slight tendency for the target to be more detectable in the vertical and horizontal orientations, but ϵ_t is negative and large for all orientations.

In all experiments the observers were given full knowledge of the geometry of the target, its place and orientation. The notion that the visual system acts as a flexible, narrow-beam scanner with respect to space can be made to account for the departures from theoretical prediction when used in conjunction with an element contribution hypothesis. A direct test of this has been performed by measuring the detectability of the 1x64 rectangle in the horizontal and vertical orientation with full knowledge of orientation on the part of the observer and, in another series, with the orientation on any trial determined randomly. No effect due to knowledge of orientation was measureable. Thus a simply hypothesis of this nature must be discarded.

Another assumption of the theory, that detection is determined solely by the height of the excitation distribution at the center, may hold the answer. If detection is determined in part by the area

of the excitation distribution which is near the criterion level, then the relatively high detectability of the rectangular targets and the relatively low detectability of the multiple-legged targets, can be understood. This possibility deserves further consideration.

Finally it may be that an understanding of the data will develop through considerations of signal and noise in the central nervous system. Noise is seldom ordered in a long, thin array, for example, and it may be that a signal of this type has an advantage over isotropic neural signal displays.

REFERENCES

1. Kincaid, W. M., Blackwell, H. R., and Kristofferson, A. B., "A Neural Formulation of the Effects of Target Size and Shape upon Visual Detection", University of Michigan, Engineering Research Institute Report 2144-280-T (in press)

2. Kristofferson, A. B. and Blackwell, H. R., "The Effects of Target Size and Shape on Visual Detection: I. Continuous Foveal Targets at Moderate Background Luminance", University of Michigan, Engineering Research Institute Report 2144-279-T (in press)

3. Ricco, Ann. Ottal., Pavis, 3A, VI, 373 (1877)

4. Brown, H. R., and Niven, J. I., "The Relation between the Foveal Intensity Threshold and Length of an Illuminated Slit", J. Exp. Psychol. 34, 464-476 (1944)

5. Fry, G.A., "The Relation of the Configuration of a Brightness Contrast Border to its Visibility", J. Opt. Soc. Amer. 37, 166-175 (1947)

6. Lamar, E.S., Hecht, S., Hendley, C.D., and Shlaer, S., "Size, Shape, and Contrast in Detection of Targets by Daylight Vision: II. Frequency of Seeing and the Quantum Theory of Cone Vision", J. Opt. Soc. Amer. 38,741-755 (1948)

7. Nachman, M., "The Influence of Size and Shape on the Visual Threshold of the Detectability of Targets", Boston Univ. Opt. Res. Lab. Tech. Note 109 (1953)

8. Blackwell, H.R., "Brightness Discrimination Data for the Specification of Quantity of Illumination", Illum. Eng. N.Y.,47 602-609 (1952)

9. Blackwell, H.R., Psychophysical Thresholds: Experimental Studies of Methods of Measurement, Univ. of Michigan Engineering Research Institute Bull. No. 36, 227 p. (1953)

10. Blackwell, H.R., Pritchard, B.S., and Ohmart, J.G., "Automatic Apparatus for Stimulus Presentation and Recording in Visual Threshold Experiments", J. Opt. Soc. Amer. 44, 322-326 (1954)

11. Kincaid, W.M., and Blackwell, H.R., "Application of Probit Analysis to Psychophysical Data: I. Techniques for Desk Computation", Univ. of Michigan, Engineering Research Institute Report 2144-283-T (in press)

TABLE I

Chronological Order of Experiments

FIRST EXPERIMENTAL ROOM

CIRCLES Series 1	RECTANGLES Series 1	CIRCLES Series 2	RECTANGLES Series 2

SECOND EXPERIMENTAL ROOM

RECTANGLES Series 3 (Circles)	CROSSES (Circles)	SPOKES (Circles)	GEOMETRICAL FIGURES (Circles)

TABLE II

Goodness of Fit of Psychophysical Data to a Normal Ogive

Observer	χ^2	Degrees of Freedom	Probability
LP	353.38	336	.248
AK	310.93	348	.924
AM	422.08	348	.004
NS	385.35	342	.052

TABLE III

Average Data for Circular Targets

Nominal Target Diameter	Log A	Log $\dot{C}$	Log $\dot{C}_c$
1'	-.14	.734	.730
2'	.42	.162	.174
4'	1.09	-.393	-.400
8'	1.66	-.738	-.741
16'	2.22	-.961	-.958
32'	2.80	-1.119	-1.114
64'	3.35	-1.238	-1.243

2455-11-F

TABLE. IV

Average Data for Rectangular Targets

Nominal Target Dimensions	log β	log α	log A	log $\dot{C}$	log $\dot{C}_c$	log $\dot{C}_t$
1x1	- .06	- .078	- .141	.777	.733	.731
2x2	.228	.22	.451	.206	.146	.151
4x4	.509	.502	1.011	- .257	- .334	- .334
8x8	.828	.822	1.650	- .705	- .735	- .729
16x16	1.107	1.103	2.210	- .936	- .955	- .947
32x32	1.410	1.410	2.820	-1.129	- 1.118	-1.117
64x64	1.711	1.709	3.420	-1.221	- 1.245	-1.241
1x2	.226	- .056	.170	.368	.421	.416
2x4	.518	.222	.740	- .100	- .123	- .111
4x8	.792	.489	1.281	- .489	- .534	- .505
8x16	1.098	.813	1.911	- .849	- .850	- .831
16x32	1.401	1.100	2.501	-1.053	- 1.042	-1.027
32x64	1.701	1.400	3.101	-1.235	- 1.184	-1.179
1x4	.526	- .056	.470	.182	.126	.157
2x8	.797	.203	.594	- .261	- .341	- .261
4x16	1.083	.487	.596	- .587	- .695	- .613
8x32	1.405	.805	2.210	- .933	- .955	- .876
16x64	1.700	1.100	2.800	-1.118	- 1.118	-1.064
1x8	.792	- .032	.760	.020	- .149	- .045
2x16	1.103	.197	1.300	- .442	- .546	- .335
4x32	1.406	.514	1.920	- .766	- .846	- .668
8x64	1.704	.786	2.490	-1.079	- 1.037	- .893
1x16	1.087	- .087	1.000	- .039	- .341	- .061
2x32	1.411	.249	1.660	- .588	- .741	- .421
4x64	1.700	.500	2.200	- .849	- .955	- .673
1x32	1.393	- .063	1.330	- .202	- .558	- .124
2x64	1.721	.239	1.960	- .572	- .868	- .432
1x64	1.738	- .058	1.680	- .345	- .756	- .153

2455-11-F

TABLE V

Average Data for Multiple-legged Targets

	Nominal Target	log A	log α'	log β'	log $\dot{C}$	log $\dot{C}_c$	log $\dot{C}_t$
Crosses	1x64, 90°	2.07	1.761	1.761	- .410	- .908	- .503
	1x64, 60°	2.03	1.703	1.761	- .334	- .893	- .460
	1x64, 24°	2.03	1.386	1.761	- .422	- .893	- .468
	1x64, 22.5°	1.99	1.347	1.748	- .450	- .879	- .397
	1x64, 10°	2.00	1.020	1.740	- .530	- .883	- .356
	1x64, 3 legs	1.93	1.641	1.703	- .368	- .857	- .366
	1x64, 6 legs	2.22	1.700	1.758	- .389	- .958	- .631
1x32 Spokes	4 legs, 90°	1.78	1.461	1.461	- .537	- .795	- .610
	4 legs, 60°	1.79	1.406	1.460	- .505	- .800	- .605
	4 legs, 45°	1.77	1.325	1.461	- .494	- .791	- .591
	4 legs, 24°	1.78	1.100	1.460	- .584	- .795	- .597
	2 legs	1.57	.623	1.460	- .523	- .695	- .572
	8 legs	2.02	1.458	1.458	- .595	- .890	- .724
1x64 Spokes	4 legs, 90°	2.06	1.755	1.755	- .524	- .904	- .613
	4 legs, 60°	2.04	1.704	1.763	- .484	- .897	- .628
	4 legs, 45°	2.07	1.620	1.763	- .534	- .908	- .608
	4 legs, 24°	2.07	1.388	1.762	- .527	- .908	- .626
	2 legs	1.80	.620	1.763	- .504	- .804	- .531
	8 legs	2.33	1.763	1.763	- .534	- .991	- .750

TABLE VI

Average Data for Geometrical Figures

Target	log A	log α'	log β'	log $\dot{C}$	log $\dot{C}_c$	log $\dot{C}_t$
Diamond	2.81	1.470	1.645	-1.101	-1.118	-1.120
Cross	2.80	1.531	1.531	-1.093	-1.116	-1.109
Hexagon	2.81	1.438	1.490	-1.102	-1.118	-1.124
Star	2.81	1.626	1.689	-1.009	-1.118	-1.107
Square	2.80	1.405	1.405	-1.097	-1.116	-1.121
Triangle	2.80	1.524	1.587	-1.103	-1.116	-1.115

2455-11-F

TABLE VII

Average absolute deviation, $\bar{\epsilon}_c$, and algebric average deviation, $|\bar{\epsilon}_c|$, of threshold contrasts for non-circular targets from threshold contrasts for equal-area circular targets. Logarithmic unit differences.

	Circular	Rectangular	Multiple-legged	Geometric Forms
$\bar{\epsilon}_c$	- .000	.086	.379	.033
$\lvert\bar{\epsilon}_c\rvert$	.006	.098	.79	.033

2455-11-F

TABLE VIII

Residual Errors, Empirical Analysis

	Circles	Rectangles	Multiple-legged	Geometrical Figures	Mean
$\bar{\epsilon}_c$	- .000	.004	.002	- .024	.000
$\lvert\bar{\epsilon}_c\rvert$	.006	.035	.054	.032	.037

TABLE IX

Errors of Prediction from Theory

	Circles	Rectangles	Multiple-legged	Geometrical figures	Mean
$\bar{\epsilon}_t$	- .000	- .042	.073	.032	.007
$\lvert\bar{\epsilon}_t\rvert$	.006	.065	.097	.032	.065

TABLE X

Residual Errors, Theoretical Analysis

	Circles	Rectangles	Multiple-legged	Geometrical Figures	Mean
$\bar{\epsilon}_t$	- .000	.007	.006	.029	.008
$\lvert\bar{\epsilon}_t\rvert$	.006	.035	.063	.030	.040

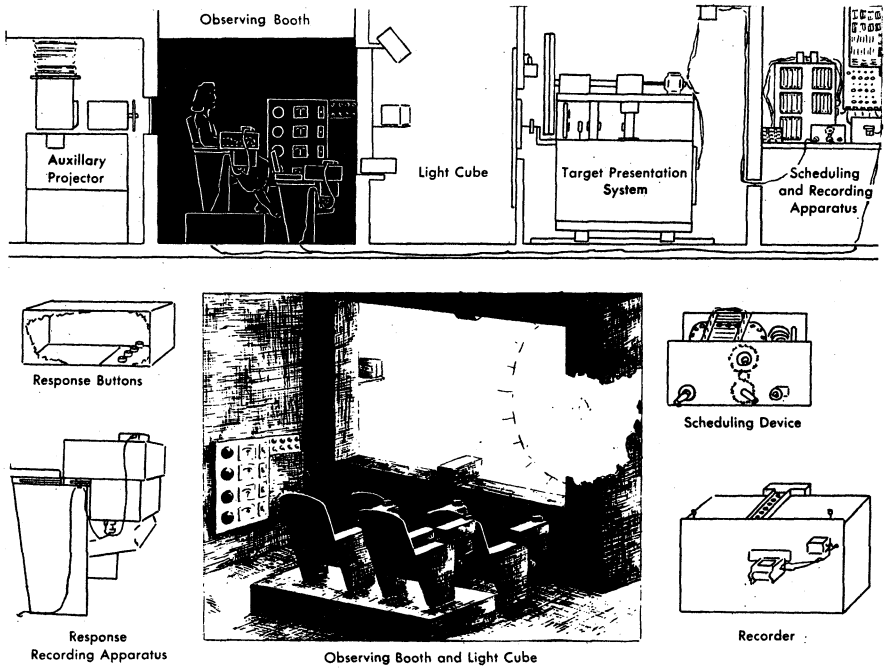

Fig. 1. Artist's conception of the basic psychophysics test facility.

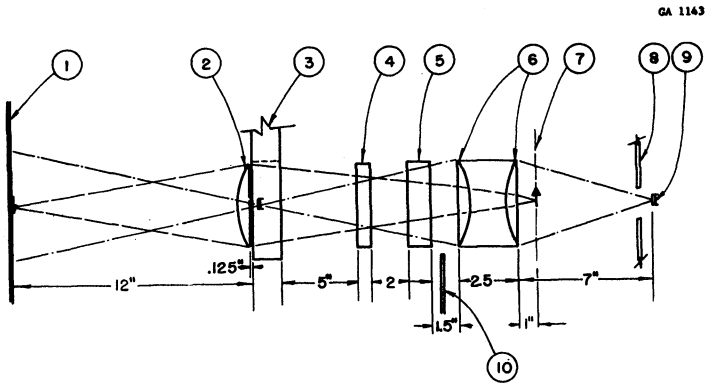

Fig. 2. Optical schematic drawing of the target projector.

64 R MULTIPLE LEG TARGETS

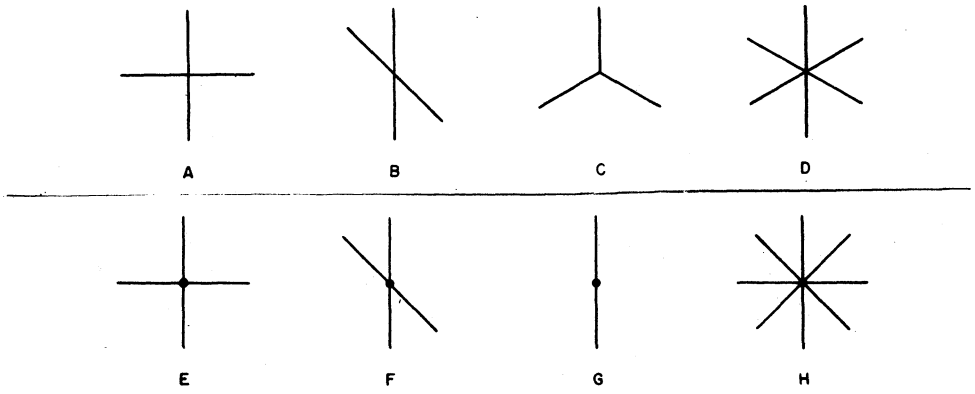

Fig. 3. Multiple-leg targets.

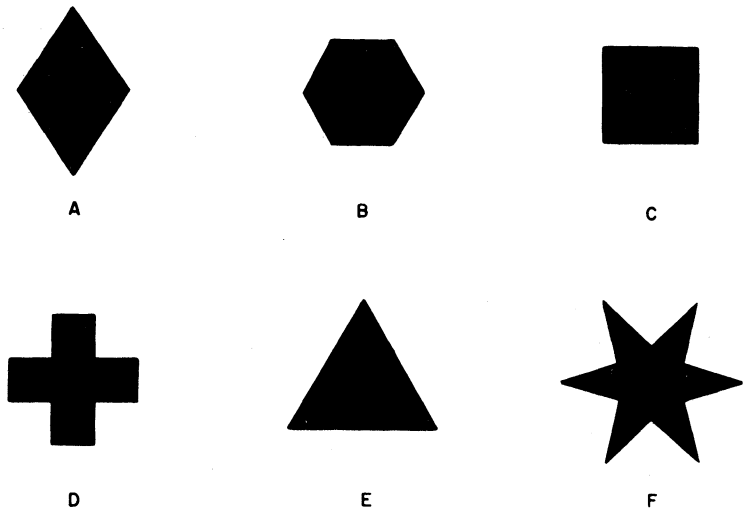

Fig. 4. Geometrical form targets.

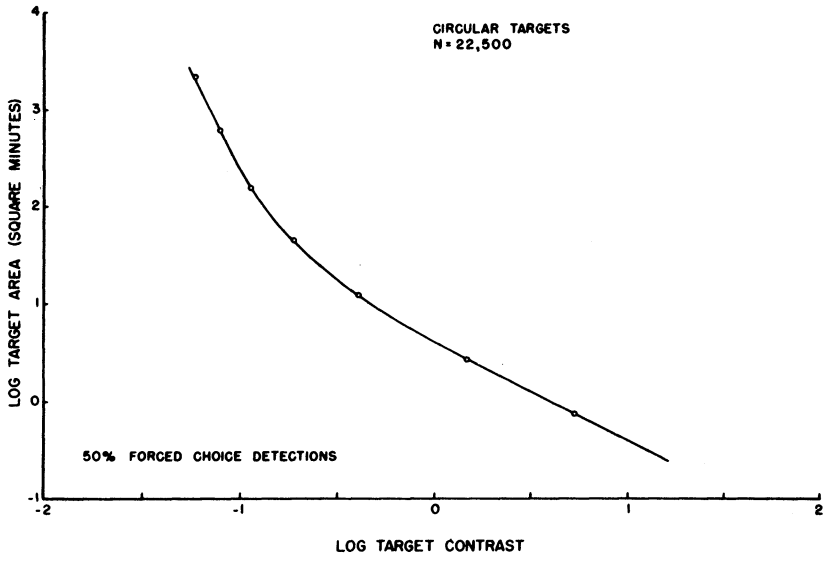

Fig. 5. Threshold data for circular targets.

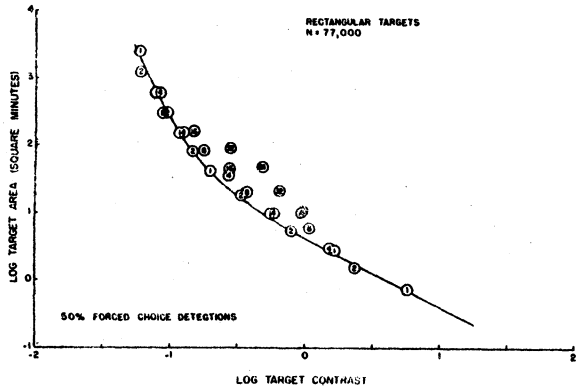

Fig. 6. Threshold data for rectangular targets.

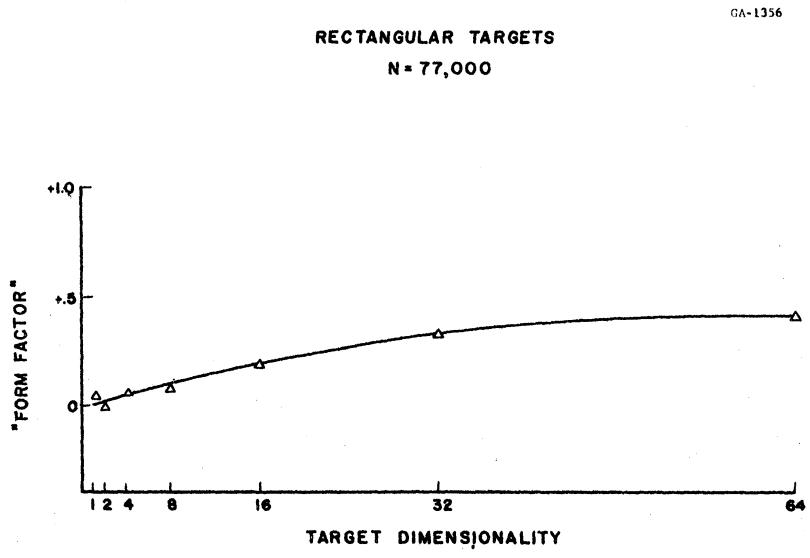

Fig. 7. Form factor graph.

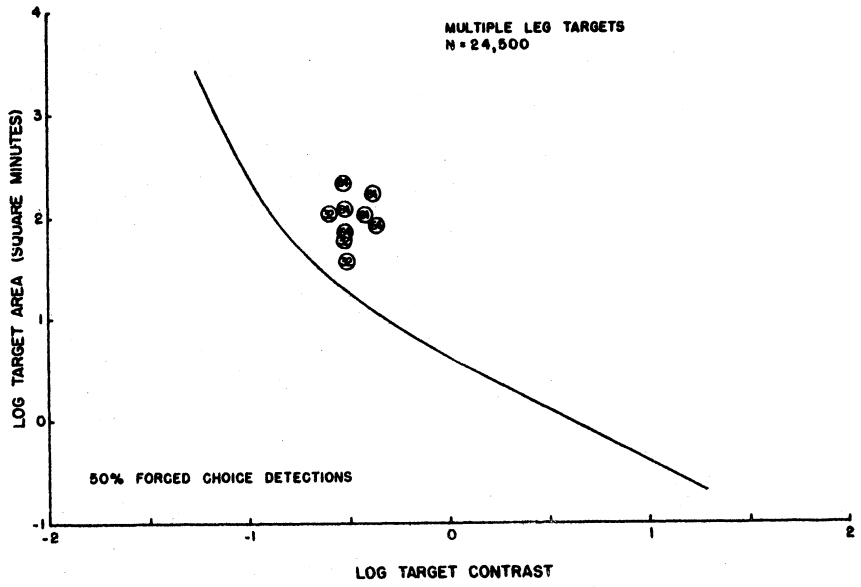

Fig. 8. Threshold data for multiple-leg targets.

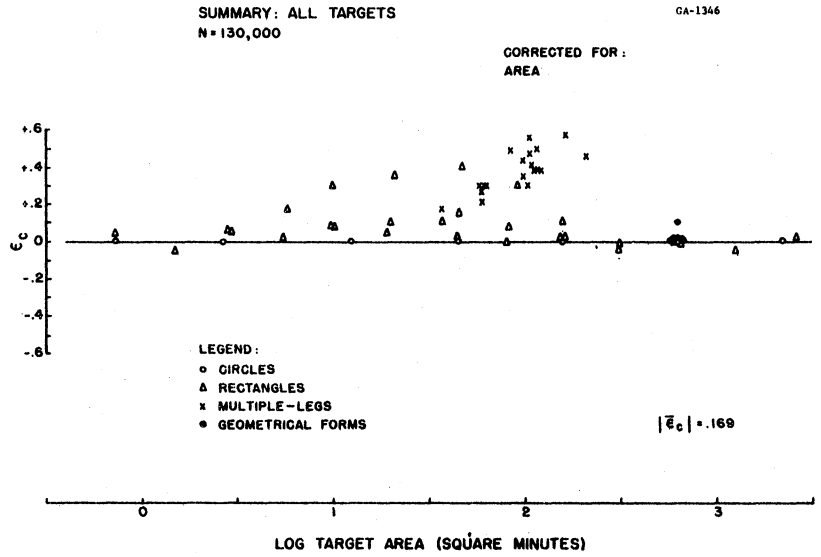

Fig. 9. Summary data analysis.

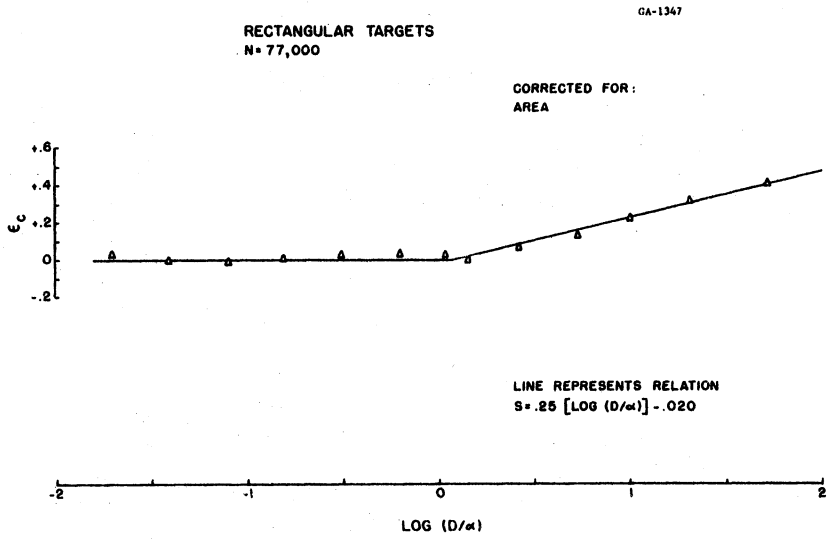

Fig. 10. Empirical shape factor.

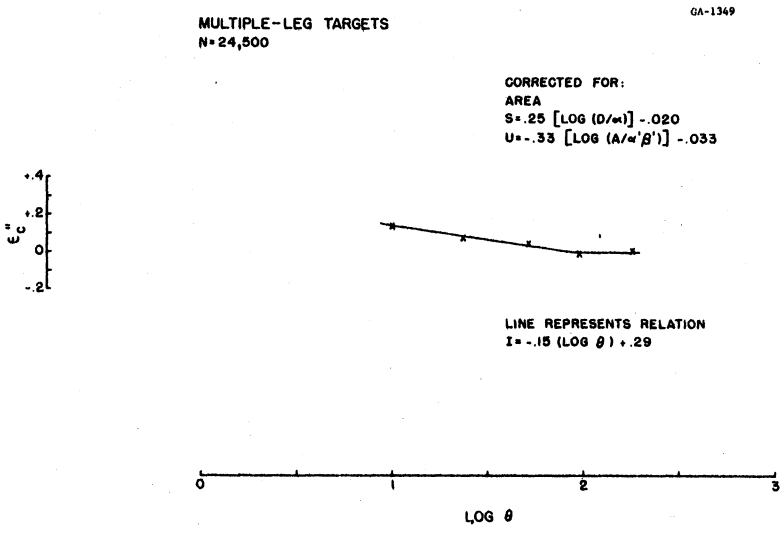

Fig. 11. Empirical inhibition factor.

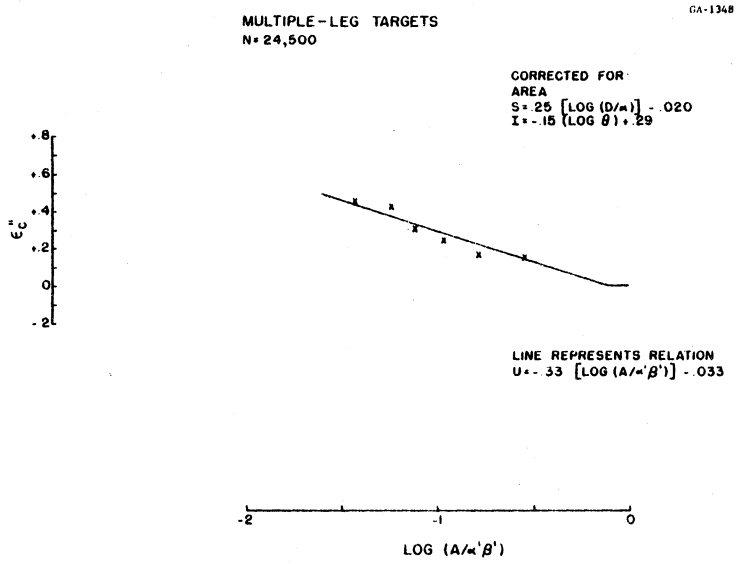

Fig. 12. Empirical utilization factor.

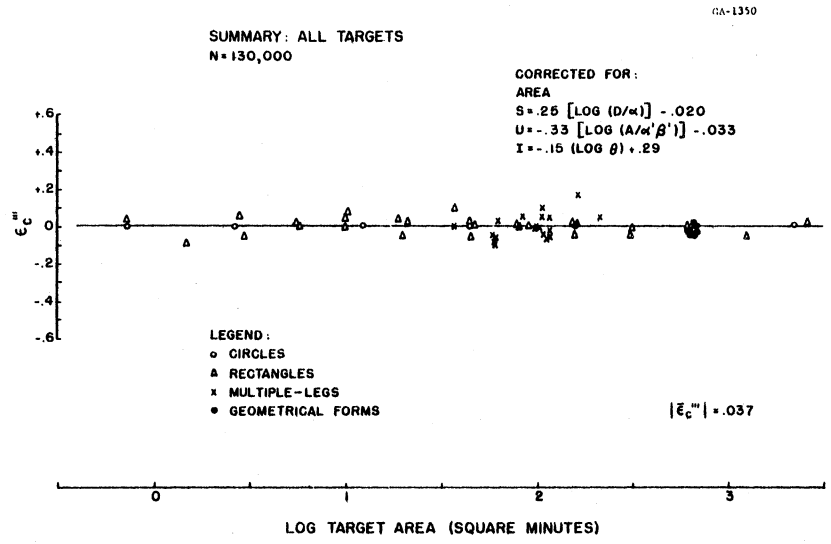

Fig. 13. Summary data analysis.

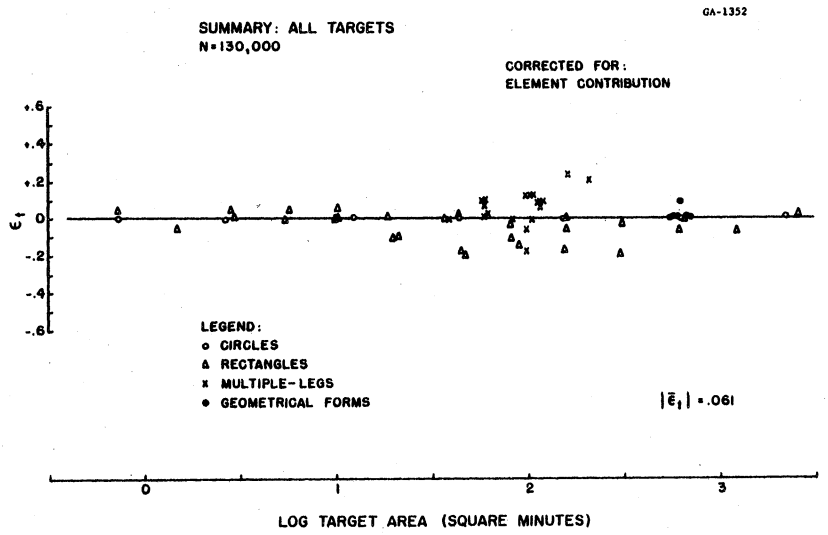

Fig. 14. Summary data analysis.

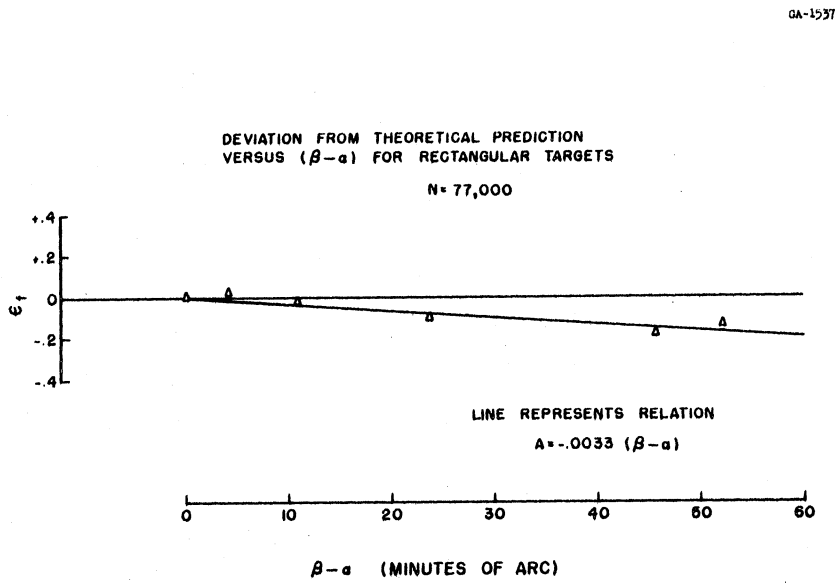

Fig. 15. Empirical asymmetry factor.

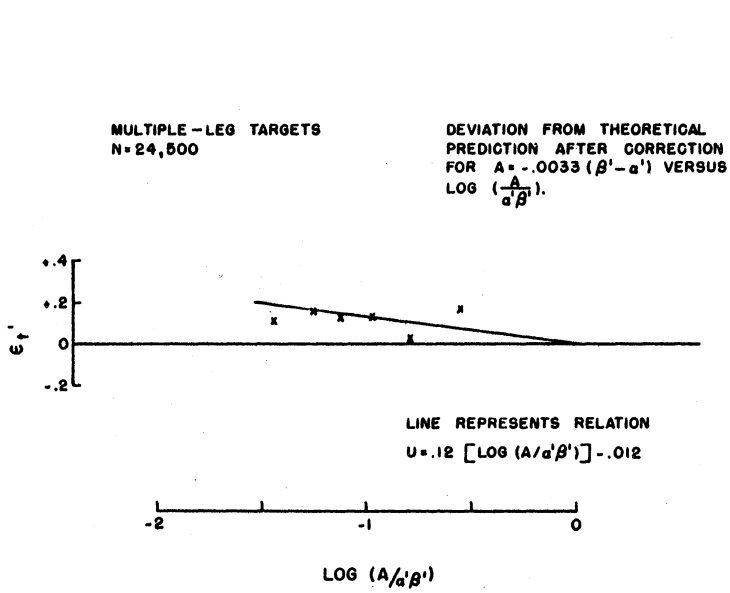

Fig. 16. Empirical utilization factor.

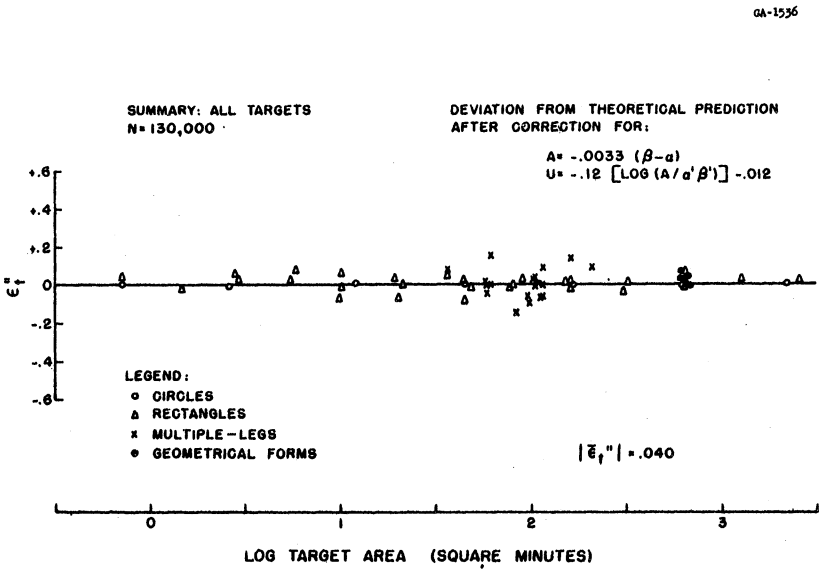

Fig. 17. Summary data analysis.

THE UNIVERSITY OF MICHIGAN